Analyzing building envelope retrofit strategies using a neural network model based on sensor data

Chirag Deb[1,*], Zhonghao Dai[1], Arno Schlueter[1]
[1]Architecture and Building Systems, Institute of Technology in Architecture, ETH Zurich, Switzerland
* Corresponding Author: deb@arch.ethz.ch

Abstract

This study presents a black-box model to analyze retrofit strategies on the building envelope of a single-family residence in Switzerland. The model is a Long-short term memory-based Recurrent neural network (LSTM-RNN) developed on data from a wireless sensor network (WSN). The 39 measured variables are filtered using a two-step feature selection process. The selected features are fed as inputs to the LSTM-RNN model that predicts the hourly heating energy consumption as an output with an accuracy of 81.24 %. A detailed significance analysis ranks the various inputs according to their order of significance. Based on this significance, we analyse the cost-optimal retrofit solution and compare it with the conventional process of exhaustive search. The cost calculations are based on the annuity method using data from a retrofit matrix of various insulation materials. We see that the proposed methodology with machine learning-based significance analysis results in a better retrofit strategy selection.

Introduction

Energy consumed in the building sector accounts for about 40 % of the total energy consumption in the developed countries. Retrofitting existing buildings is vital to increase the efficiency of the building stock as buildings have a long life span (Deb and Lee, 2018). To realise this goal, accurate energy assessment methods for retrofitting existing buildings are required. The core of such assessment methods is the development of energy models of buildings (Deb and Schlueter, 2021). This article focuses on applying machine learning methods to model thermal dynamics of an individual building with a view to use this model for retrofit analysis.

At present, methods for energy modelling of buildings can be mainly categorized as white-box, grey-box and black-box methods (Amasyali and El-Gohary, 2018). White-box models have popularly been used for retrofit analysis (Guardigli et al., 2018; Ascione et al., 2017; Yuan et al., 2019; Chen et al., 2017). However, white-box model relies on principles of building-physics and requires information which are often difficult to obtain (Zhao and Magoulès, 2012). On the other hand, grey-box models combine physics-based models with in-situ measurements. A popular example of such methods are the resistance-capacitance models that use electrical analogies for thermal modelling of buildings (Bacher and Madsen, 2011; De Rosa et al., 2014; Brastein et al., 2018). The in-situ measurements are used to calibrate these models with the aim to find the model parameters and to capture the model uncertainties.

In contrast, black-box models only rely on measured data. The main advantage here is that these do not require any prior knowledge and can directly be trained with measured data. These models allow to handle complicated system dynamics without getting involved in system intricacies. In addition, these models can be re-trained and updated with new data. This enables the model to capture uncertain changes and adapt to the changing system while also allowing for automation of this entire process. The black-box models are usually based on statistical and machine learning techniques (Guo et al., 2018), such as simple linear regression(LR) (Foucquier et al., 2013; Friedrich and Afshari, 2015), multiple linear regression(MLR) (Fumo and Biswas, 2015; Massana et al., 2015; Fan et al., 2014; Guo et al., 2018) and support vector regression(SVR) (Foucquier et al., 2013; Fan et al., 2014; Wang et al., 2018; Guo et al., 2018; Dong et al., 2005; Jain et al., 2014).

Recent years have witnessed the rise of deep neural networks like recurrent neural network (RNN) in the domain of building energy modelling. Their ability in building energy prediction usually outperforms traditional machine learning methods as these are made of time-dependent units that are useful in analysing time series data (Guo et al., 2018). Researchers have also incorporated long short-term memory (LSTM) with RNNs to address the gradient problem during the training stage (Hochreiter and Schmidhuber, 1997). Building energy demand and consumption can also be predicted with LSTM-RNN with sequence architecture (Marino et al., 2016). Rahman et al. (2018) utilised RNN with a LSTM unit to predict the electricity consumption for both commercial and residential buildings and noted that the RNN model can also

deal with missing values. However, the use of recurrent neural network in predicting energy consumption has been limited and no study has used it for retrofit analysis.

With this view, this study will establish a thermal dynamic model using RNN and analyze building envelope retrofit strategies purely based on sensor data. Prior to this, a systematic feature selection is performed that selects the relevant features (or measured variables) that are fed as inputs to the RNN model. To compensate the general difficulty of interpreting machine learning models, we perform a significance analysis on the features (Lundberg and Lee, 2017). This gives a clear understanding of the building elements that are most significant to the model and are most crucial for retrofitting. This is the main novelty of the paper, where machine learning-based significance analysis is used to determine the cost-optimal retrofit solution. Finally, we compare the results to the conventional approach where exhaustive search is used to determine the cost-optimal solution and discuss the merits of the proposed method.

Methods

The RNN model is developed on measurements from wireless sensor network (WSN) in a single-family residence in Switzerland. The details of the WSN and its applications can be seen in Frei et al. (2020); Deb et al. (2020, 2019) The house has a total energy reference area of 144 m^2. The building is located in a sunny, unobstructed location, contains six rooms, and is occupied by a family of two adults. It has three storeys with the façade made of modular bricks and the floors made of concrete. The facade is composed of 32 cm modular brick with 1.5 cm each of inner and outer plaster. The estimated U-value of the masonry is 1.07 W/m^2K. The windows have a wooden-metal frame with double-glazing. The estimated U-value of the two window systems is 1.6 and 2.4 W/m^2K respectively. It has a flat roof made of concrete with layers of vapor barrier, mats, bitumen and gravel. The estimated U-value of the roof is 0.46 W/m^2K. The space heating system consists of an oil-based boiler and a combination of radiators and an underfloor heating network (for the expanded living room). The temperature setting of the space-heating system is same for the weekdays and the weekends. The settings are not altered by the occupants. The temperature settings are fixed at 21°C between 9:00 and 20:00 and 15°C between 20:00 and 9:00. The space heating network has no thermal storage. The loop for underfloor heating also contains a mixing valve. The heating system has a power rating of 24kW. The measurements took place between February and April of 2019. A total of 37 sensors were installed that recorded hourly values for various variables which can be classified into the following six categories:

- Indoor air temperature and relative humidity
- Oudoor air temperature
- Supply/return temperature of the heating system and the radiators
- Heat flux through the windows and the walls (also used to calculate the U-values)
- Window opening time
- CO_2-concentration
- Energy-related: Electricity, oil consumption, flow Meter for hot water for space heating

The WSN layout and measurement information can be seen in Table 7 and Table 8 in the Appendix.

Feature selection

This study uses a two-step feature selection procedure based on correlation strength (Amjady et al., 2011). Correlation strength metric includes Pearson correlation, Spearman correlation and mutual information. There are a total of 48 input features generated from hourly WSN measurements. It should be noticed that the *Flow_meter*, the *Return_temp_6* and the *Supply_temp_6* are removed as they are used to derive the heating demand. The *Return_temp_7*, *Supply_temp_7*, *Return_temp_21* and *Supply_temp_21* are also removed prior to the feature selection as these measure the hot water temperature from the space heating system and are considered to be highly correlated to *Return_temp_6* and *Supply_temp_6*. The heating demand is calculated using measurements of the supply and return temperature of hot water for space heating and the flow rate.

The feature selection process involves two steps - the relevancy and the redundancy filters. The relevancy filter removes irrelevant features in predicting the heating demand while redundant features remove highly correlated features for dimension-reduction. The results of the feature selection is shown in Figure 1.

Long Short Term Memory(LSTM)-RNN

RNN captures and remembers the dependency among consecutive input features within the RNN hidden state. To improve the vanishing gradients problem, RNN with long short-term memory (LSTM) units is proposed by Hochreiter and Schmidhuber (1997).

The mathematical formula for the LSTM unit is as in equation 1.

$$\begin{aligned} f_t &= \sigma_g\left(W_f x_t + U_f h_{t-1} + b_f\right) \\ i_t &= \sigma_g\left(W_i x_t + U_i h_{t-1} + b_i\right) \\ o_t &= \sigma_g\left(W_o x_t + U_o h_{t-1} + b_o\right) \\ c_t &= f_t \circ c_{t-1} + i_t \circ tanh\left(W_c x_t + U_c h_{t-1} + b_c\right) \\ h_t &= o_t \circ tanh\left(c_t\right) \end{aligned} \tag{1}$$

where σ_g is sigmoid function and $\circ$ denotes Hadamard product (matrix element multiplication). The variables in the equation above can be tabulated as in Table 1.

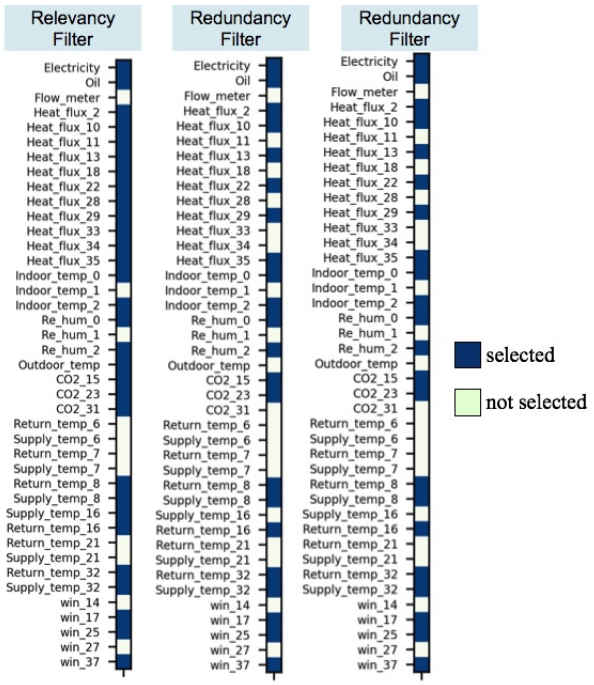

Figure 1: Two-step feature selection using mutual information as the metric.

$x_t \in \mathbb{R}^d$	input
$f_t \in \mathbb{R}^h$	forget gate's activation
$i_t \in \mathbb{R}^h$	input gate's activation
$o_t \in \mathbb{R}^h$	output gate's activation
$h_t \in \mathbb{R}^h$	hidden state
$c_t \in \mathbb{R}^h$	cell state

Table 1: Variables in the LSTM model.

Attention Mechanism

We introduce an attention mechanism as an additional layer in the LSTM-RNN model. Attention mechanism is put forth by Luong et al. (2015). Since the RNN model in this paper is a many-to-one model, the attention mechanism enables measurements from previous time steps as inputs to the model while the heating demand (output) is predicted at the current timestamp. This model architecture can be visualized as in Figure 2. We use dot product to calculate the scores for the attention mechanism. Therefore, the importance score β_i for each time step i can be calculated as in equation 2.

$$\beta_i = \frac{\boldsymbol{u}^\top \tanh\left(\boldsymbol{W}\left[\boldsymbol{o}_t\right]\right)}{\sum_{i=1}^{t} \boldsymbol{u}^\top \tanh\left(\boldsymbol{W}\left[\boldsymbol{o}_t\right]\right)} \tag{2}$$

The weighted sum of the output state from the LSTM Layer 2 is denoted as an encoder for consecutive measurements and used to predict the target variable at time t. The encoder is calculated as in equation (3). It's assumed that this encoder contains the information from previous time step to predict current heating demand.

$$Encoder = \sum_{i=1}^{t} \beta_i * \boldsymbol{o}_i \tag{3}$$

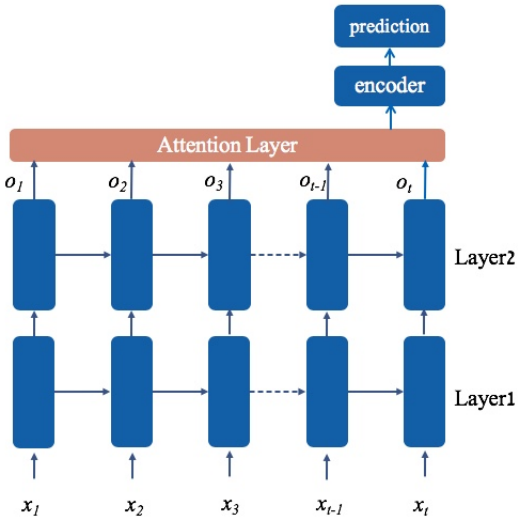

Figure 2: The LSTM model with an attention mechanism.

Significance Analysis: SHAP Value

SHAP (SHapley Additive exPlanations) is a tool aimed to explain the importance of input features in black-box models (Lundberg and Lee, 2017). In order to calculate the effect of including or excluding a feature i, a model $f_{S\cup\{i\}}$ with feature i and a model f_S without i should be trained. Further, the prediction difference from these two models are calculated as $f_{S\cup\{i\}}\left(x_{S\cup\{i\}}\right) - f_S\left(x_S\right)$, where x_S represents input feature values in set S. Finally, the classical shapley value is defined as a weighted average of all the possible differences. As the computation of classical shapley is time and computational-intensive, SHAP values are introduced as conditional expectation function of the original model (equation 4).

$$\phi_i(f,x) = \sum_{z'\subseteq x'} \frac{|z'|!\,(M-|z'|-1)!}{M!}\left[f_x\left(z'\right) - f_x\left(z'\backslash i\right)\right] \tag{4}$$

A larger absolute SHAP value ϕ_i for feature i in the model indicates the relative high-importance of this feature. Once the LSTM-RNN model is ready, we will test the significance of the features related to building envelope retrofit strategies using SHAP values.

Retrofit Analysis

The retrofit analysis entails testing different retrofit measures on the different parts of the building envelope - the roof, the floor, the walls and the windows. The cost-optimal solution is the one that corresponds to minimum life-cycle costs while resulting in a reasonable energy consumption. The data on costs and properties of the retrofit measures is taken from Sigrist (2018); Sigrist et al. (2019). Table 10 (in the appendix) shows the different measures for retrofitting the building envelope. Once the thermal dynamic model for the house is established, the rela-

tion and sensitivity between energy consumption and the input features is assumed to be fixed. Then, the new input features determined by retrofit measures will be generated and used in the LSTM-RNN prediction model. For example, heat flux for a retrofit retrofit measure on the envelope can be synthesized as in equation 5. The indoor and the outdoor temperature are assumed to remain the same for retrofit analysis. This is one of the advantages of this data-driven approach where time series data on indoor air temperature captures the occupant-induced variation and the same is assumed post-retrofit.

$$\begin{aligned} \textit{Heat Flux} = U_value_{new} \times \\ (\textit{Indoor Temperature} - \textit{Outdoor Temperature}) \end{aligned} \quad (5)$$

Furthermore, the distribution of generated new heat flux will be examined to ensure it is still within the reasonable range as the heat flux used when training the model, which is the fundamental for machine learning techniques.

Retrofit Cost Calculation

The life cycle cost for a retrofit measure is composed of three components: investment, operation& maintenance and energy cost. Using the annuity method, all costs are converted into constant annual payments, called annuities. The investment cost A_{inv} can be calculated by multiplying the initial investment cost with the discount rate (equation 6).

$$A_{inv} = I * \frac{r * (1+r)^n}{(1+r)^n - 1} \quad (6)$$

where I is the initial investment cost, r is the interest rate and n is the lifetime. It is assumed that operation& maintenance cost $A_{o\&m}$ are constant annual costs. The energy cost A_{energy} is calculated directly from heating consumption $E_{heating}$ times electricity price P_e (equation 7).

$$A_{energy} = E_{heating} \times P_e \quad (7)$$

where $E_{heating}$ is defined as in equation 9. The price of electricity is assumed to be 0.21 [CHF/kWh] as the average price between 2010 and 2050 as per Almeida and Ferreira (2017).

Therefore, annual cost A_{tot} for the different retrofit measures is calculated as (equation 8):

$$A_{tot} = A_{O\&M} + A_{inv} + A_{energy} \quad (8)$$

After predicting the heating demand $D_{heating}$ from the LSTM-RNN model, the heating consumption $E_{heating}$ can be calculated as in equation 9:

$$E_{heating} = D_{heating}/\eta_{hs} \quad (9)$$

where η_{hs} is efficiency for different heating system. The primary energy consumption can be calculated by multiplying the heating consumption with the energy factor. The energy factor depends on the primary heating source used for heating system and is shown in Table. 2 ((Sigrist, 2018)). Using these factors, the primary energy consumption $E_{primary}$ is derived as in equation 10.

Energy carrier	Primary energy factor [kWh/kWh]
Oil	1.24
Wood pellets	1.20
District heating(Swiss average)	0.87
Electricity(Swiss consumer mix)	3.00

Table 2: Energy factor for the various energy sources.

MAPE(%)	Pearson	Spearman	Mutual Info.
LSTM-RNN	22.35	20.50	**18.76**

Table 3: Results for the testing data set for predicting the heating demand.

$$E_{primary} = E_{heating} \times factor = D_{heating}/\eta_{hs} \times factor \quad (10)$$

Result

Model Accuracy

The data are split into the training, validation and the testing set by 80%, 10%, 10%. We apply early stop and dropout (Srivastava et al., 2014) to avoid over-fitting. The early stop terminates the training when the validation does not decrease anymore. The mean absolute prediction error (MAPE) for the LSTM-RNN model on the test set is shown in Table.3. The three columns correspond to the three feature selection processes. We see that the LSTM-RNN model with features selected through mutual information has the best prediction result. This improvement is attributed to the ability of the mutual information to capture relationship and mutual dependence among the variables although these may not be linearly correlated. The other two feature selection metrics do not capture non-linear dependencies.

Figures 3 and 4 show the predicted heating demand from the LSTM-RNN model versus the measured data. As shown in this figure, the model has a good prediction performance except when the heating demand is large. This trained LSTM-RNN model will be further utilized for retrofit analysis.

Significance Analysis

In order to explain the significance of each input feature when predicting demand SHAP analysis is applied. With the SHAP package, it is possible to visualize the feature's impact on the heating demand in every time step. It also shows whether the rela-

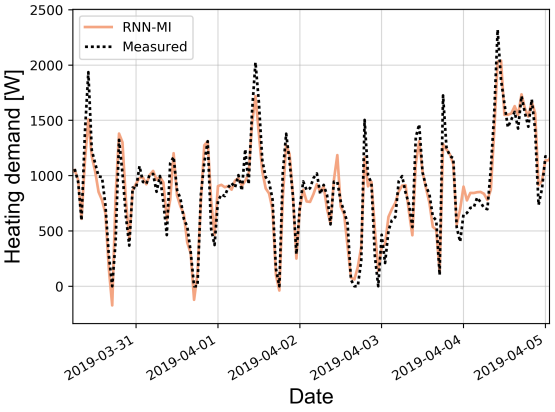

Figure 3: Measured vs predicted time series of the heating demand resulting from the LSTM-RNN model.

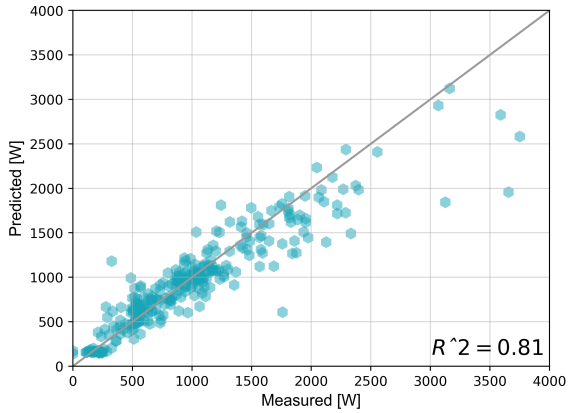

Figure 4: Scatter plot for the measured vs predicted values resulting from the LSTM-RNN model.

tionship is positive or negative. For example, Figure 5 shows SHAP values for each input feature at time step t and $t-4$. Compared with Figure 5a and Figure 5b (notice the different x-axis scale in two figures), input feature values at previous time step are less important than the current values.

In this case, more attention should be focused on SHAP values at time step t. The input features are already sorted by their SHAP values in Figure 5. For retrofitting analysis with regards to the building envelope, only features related to the envelope properties are of concern. These relate to those that measure heat flux through the walls and the windows. According to Figure 5b, the significance of the heating flux features can be ranked from the highest to the lowest as: *Heat_flux_22*, *Heat_flux_34*, *Heat_flux_35*, *Heat_flux_10*, *Heat_flux_11*, *Heat_flux_18*, *Heat_flux_2*, *Heat_flux_29*, *Heat_flux_33* ,*Heat_flux_13*. The details of their location can be seen in Table. 7.

Cost-optimal Retrofit Solution

There are four different categories of the building envelope that can be replaced. These are the roof, the floor, the walls and the windows. We can either re-

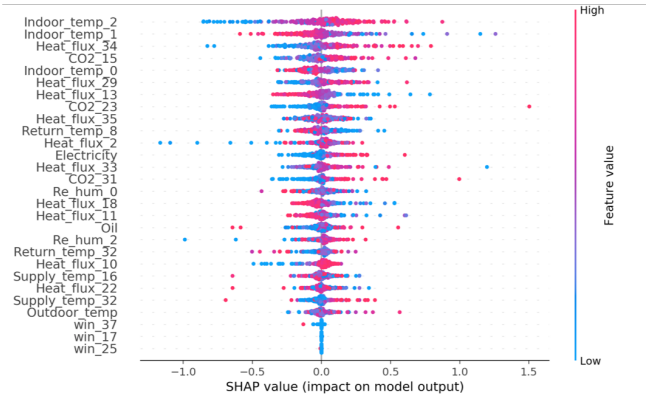

(a) SHAP values for input features at $t-4$.

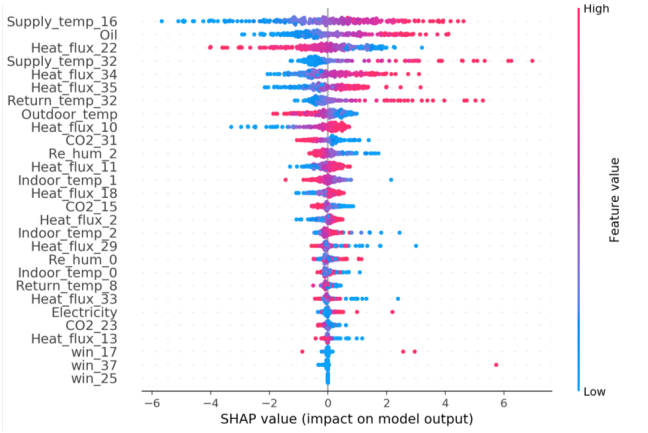

(b) SHAP values for input features at t.

Figure 5: SHAP values for each input feature at time steps t-4 and t.

place one of these types or a combination of several types. We use the data of the U-value of the building materials corresponding to each category of the envelope (Appendix Table 10) and use these to generate the time series for the heat flux. While selecting the insulation material on the walls, we use the same material for walls in all four orientations. This is a common practice in the retrofitting process. Further, we combine different types of building envelopes to find the optimal retrofitting solution. All the exhaustive combinations are examined and the results of their annual cost and primary energy consumption is shown in Figure 6. The exhaustive combinations performance search is proceeded as: replace one category building envelope with all possible materials from Table 10 , then replace two categories with all available materials until replace all four categories. In this figure, the green hexagon *RC* means reference case, which represents maintaining the current building envelope and the heating system. *1 type* corresponds to retrofitting just one category: either the roof, the walls and the windows or the cellar ceiling. *2 types*, *3 types* and *4 types* corresponds to the combination of two, three and four categories of the building envelope respectively. As we see that this exhaustive search is inefficient and does not consider

Data Description	*original Heat_flux_35*	*new Heat_flux_35*
min	-12	-0.14
25%	3.53	1.31
50 %	6.26	1.75
75%	9.87	1.75
max	23.08	3.00

Table 4: An example of the generated Heat_flux_35 for a facade insulation material, BE_3h.

the importance of the heat flux features as per the significance analysis, we consider this aspect in the next section.

As mentioned in section **Retrofit Analysis**, to ensure the reliability of retrofit result, the range for new heat flux is examined to check that the heat flux after retrofit does not deviate from the data when the model is established. For example, *Heat_flux_35*, as the data description shown in Table 4, the generated *Heat_flux_35* with BE_3h material(details in Table 10) is still within the range of heat flux used when training the model.

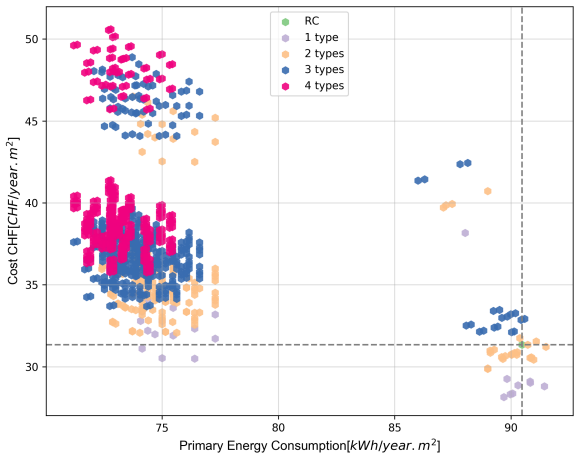

Figure 6: Results from the exhaustive combination of the envelope elements for cost-optimal retrofit analysis.

Considering Significance

Table 5 shows the significance of the heat flux and the corresponding envelope type.

To incorporate the significance, we apply a simple greedy algorithm. A simple greedy algorithm is rather intuitive and performed in the following way: uses the best insulation material for the building envelope category whose heat flux is the most significant. The next significant envelope is retrofitted with the next best insulated material and so forth. Besides, to search for the cost-optimal retrofitting solution, we offer the options as shown in Table 6.

Heat flux Ranking	Input feature	Type
1	*Heat_flux_22*	Cellar ceiling area
2	*Heat_flux_34*	Wall area
3	*Heat_flux_35*	Wall area
4	*Heat_flux_10*	Window area
5	*Heat_flux_11*	Window area
6	*Heat_flux_18*	Window area
7	*Heat_flux_2*	Cellar ceiling area
8	*Heat_flux_29*	Wall area
9	*Heat_flux_33*	Roof area
10	*Heat_flux_13*	Wall area

Table 5: Ranking of the heat flux features based on the significance analysis.

Case	Heat flux 22	Heat flux 34	Heat flux 35	Heat flux 10	Heat flux 11	Heat flux 18	Heat flux 2	Heat flux 29	Heat flux 33	Heat flux 13
1	*									
2	*	*								
3	*	*	*							
4	*	*	*	*						
5	*	*	*	*	*					
6	*	*	*	*	*	*				
7	*	*	*	*	*	*	*			
8	*	*	*	*	*	*	*	*		
9	*	*	*	*	*	*	*	*	*	
10	*	*	*	*	*	*	*	*	*	*

*Table 6: 10 cases considering significance, where * means that the corresponding envelope is retrofitted.*

In this case, each building envelope category will be retrofitted with a different material. Although it's not commonly used in retrofitting engineering, it's worthwhile to investigate the results when considering significance. From Table 6, only the most important envelope element is retrofitted for Case 1, while in Case 2, the first two most important elements are retrofitted. Similarly, Case 10 consists of retrofitting all the elements. The corresponding primary energy consumption and annual cost are shown in Figure 7. It is easy to locate the cost-optimal retrofit solution, which corresponds to that of Case 2. This corresponds to retrofitting *Heat_flux_22* and *Heat_flux_34* which are the ceiling of the basement and the east-facing wall respectively.

In this case, each envelope category will be retrofitted with a different material. Although it's not commonly used in retrofitting engineering, it's worthwhile to investigate the results when considering significance. From Table 6, only the most important envelope element is retrofitted for Case 1, while in Case 2, the first two most important elements are retrofitted. Similarly, Case 10 consists of retrofitting all the elements. The corresponding primary energy consumption and annual cost are shown in Figure 7. It is easy to locate the cost-optimal retrofit solution, which corresponds to that of Case 2. This corresponds to retrofitting

Heat_flux_22 and *Heat_flux_34* which are the ceiling of the basement and the east-facing wall respectively.

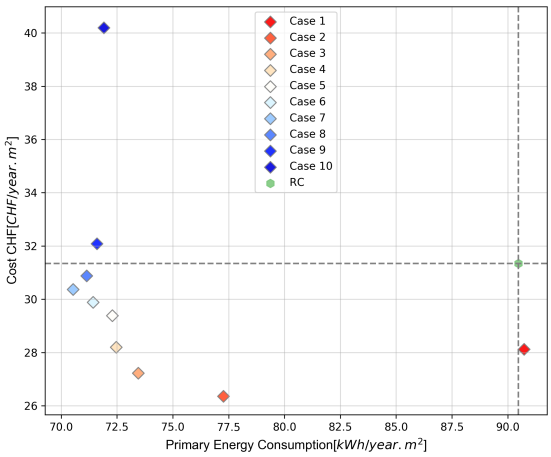

Figure 7: Cost-optimal retrofit results considering significance of the input features.

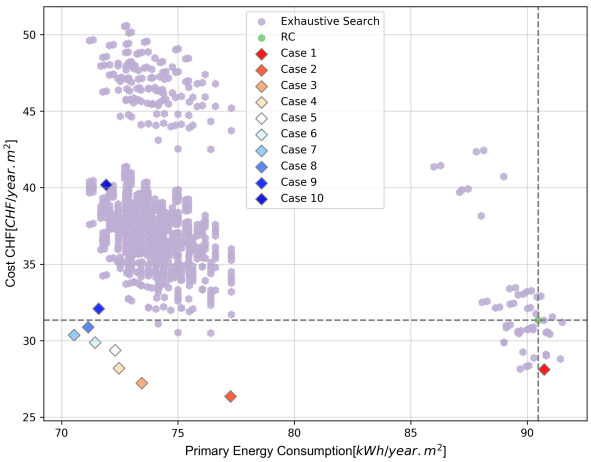

Figure 8: Comparison of the retrofit results with that from the exhaustive search.

Figure 8 shows the results from the exhaustive search and considering significance. It's worthwhile to notice that results shown in Figure 8 is exactly the same as in Figure 6 except for the color scheme. All the results from the exhaustive search are shown in one color for simplicity and 10 case study retrofitting results from significance analysis are highlighted. We see that the cost-optimal retrofitting solution remains to be Case 2 from the significance analysis. The corresponding annual cost for this strategy is $26.36 CHF/(year \cdot m^2)$ with a primary energy consumption of $77.26 kWh/(year \cdot m^2)$. Here, the *Heat_flux_22* and *Heat_flux_34* are replaced with U-values of 0.19 $kW/m^2 * K$ and 0.12 $kW/m^2 * K$ respectively (from Table 10).

Conclusion

This paper presents a cost-optimal retrofit analysis by developing a LSTM-RNN model on measured data. The feature selection process with relevancy and redundancy filters produces a LSTM-RNN model with a MAPE of 18.75 %. This result is satisfactory when compared to the high randomness in building variables and the heating energy consumption. The developed model is used to test the retrofit measures. A novel significance analysis step allows to test retrofit measures based on the importance of the input features. The results for cost-optimality are compared with that from an exhaustive search. It is promising to base the retrofit analysis solely on the significance analysis, thereby eliminating the process of exhaustive search. Significance analysis allows us to rank the envelope elements in order of their significance on the heating energy consumption. Therefore, the retrofit strategies could be appropriately assigned based on this ranking. Although the developed model is highly specific to the data set, the proposed methodology could be extended to measurements from other buildings. The limitation of the proposed retrofit strategies is that it heavily depends on the quantity and quality of WSN sensors. The energy consumption related variables should be measured and recorded with the sensor in order to ensure the modelling accuracy and therefore enhance the degree of reliability for retrofit analysis. The authors would also like to mention that since this paper was submitted, the authors have also published a detailed work on this modelling framework (Deb et al., 2021) along with another study highlighting the importance of in-situ measurements for evaluating the heat transfer coefficient in buildings (Deb et al., 2021).

Acknowledgement

This research project is financially supported by the Swiss Innovation Agency Innosuisse and is part of the Swiss Competence Center for Energy Research SCCER FEEB&D. The authors are also thankful to Mario Frei and Sigrist Diego for helping with the WSN measurements and the retrofit matrix respectively.

Appendices

WSN Node Description

Table 7 and Table 8 gathers the information for WSN sensors with their names, node numbers and sensor locations.

Table 10 is the retrofit matrix used in the paper. Each material corresponds with one type of building envelope, their U-value and the expenses.

Table 9 shows current heating system information deployed in house.

Sensor name	Sensor node number	Sensor location
Electricity	503	B, corridor
Oil	504	B, boiler room
Flow_meter	505	B, boiler room
Heat_flux_2	502	B, floor
Heat_flux_10	510	1F, living area, west glass wall
Heat_flux_11	511	1F, living area, north window
Heat_flux_13	513	1F, entrance, north wall
Heat_flux_18	518	1F, kitchen, window
Heat_flux_22	522	1B, ceiling
Heat_flux_28	606	2F, bedroom 2, window
Heat_flux_29	607	2F, bedroom 2, west wall
Heat_flux_33	611	2F, bedroom 3, roof
Heat_flux_34	612	2F, bedroom 3, east wall
Heat_flux_35	613	2F, bedroom 2, south wall
Indoor_temp_0	501	B
Indoor_temp_1	Average(509 512 519)	1F
Indoor_temp_2	Average(520 608 604)	2F
Re_hum_0	501	B
Re_hum_1	Average(512 519)	1F
Re_hum_2	Average(520 604)	2F
* B: Basement, 1F: 1st floor, 2F: 2nd floor		

Table 7: Sensor name, node number and their locations.

Sensor name	Sensor node number	Sensor location
Outdoor_temp	Average(509 608 614)	Outdoor
CO2_15	515	1F, living area
CO2_23	601	2F, corridor
CO2_31	609	2F, bedroom 2
Return_temp_6	506	B, boiler room, space heating, after heater
Supply_temp_6	506	B, boiler room, space heating, after heater
Return_temp_7	507	B, boiler room, space heating, floor heating
Supply_temp_7	507	B, boiler room, space heating, floor heating
Return_temp_8	508	B, laundry, domestic hot water
Supply_temp_8	508	B, laundry, domestic hot water
Supply_temp_16	516	1F, kitchen
Return_temp_16	516	1F, kitchen
Return_temp_21	521	1B, boiler room, space heating, radiators
Supply_temp_21	521	1B, boiler room, space heating, radiators
Return_temp_32	610	2F, bedroom 2
Supply_temp_32	610	2F, bedroom 2
win_14	514	1F, living area, west glass door
win_17	517	1F, kitchen
win_25	603	2F, bedroom 1
win_27	605	2F, bedroom 2
win_37	615	2F, bedroom 3
* B: Basement, 1F: 1st floor, 2F: 2nd floor		

Table 8: Sensor name, node number and their locations(Continued)

Code	Heating System	Investment Cost		Operation& Maintenance Cost	
		CHF	CHF/kW	CHF/year	CHF/(year*kW)
HS_0	Oil boiler	16310	133	650	0

Table 9: Heating system

References

Almeida, M. and M. Ferreira (2017). Cost effective energy and carbon emissions optimization in building renovation (annex 56). *Energy and Buildings 152*, 718–738.

Amasyali, K. and N. M. El-Gohary (2018). A review of data-driven building energy consumption prediction studies. *Renewable and Sustainable Energy Reviews 81*, 1192–1205.

Amjady, N., F. Keynia, and H. Zareipour (2011). Wind power prediction by a new forecast engine composed of modified hybrid neural network and enhanced particle swarm optimization. *IEEE transactions on sustainable energy 2*(3), 265–276.

Ascione, F., N. Bianco, C. De Stasio, G. M. Mauro, and G. P. Vanoli (2017, July). CASA, cost-optimal analysis by multi-objective optimisation and artificial neural networks: A new framework for the robust assessment of cost-optimal energy retrofit, feasible for any building. *Energy and Buildings 146*, 200–219.

Bacher, P. and H. Madsen (2011, July). Identifying suitable models for the heat dynamics of buildings. *Energy and Buildings 43*(7), 1511–1522.

Brastein, O. M., D. W. U. Perera, C. Pfeifer, and N. O. Skeie (2018, June). Parameter estimation for grey-box models of building thermal behaviour. *Energy and Buildings 169*, 58–68.

Code	Unit[m^2]	Thermal conductivity [$W/(m * K)$]	Investment costs [CHF/m^2]	U-value [$W/(m^2 * K)$]
BE_1a	Roof area	0.036	70	0.257
BE_1b	Roof area	0.036	79	0.180
BE_1c	Roof area	0.030	84	0.214
BE_1d	Roof area	0.03	95	0.150
BE_2	Roof area	0.03	407	0.044
BE_3a	Facade area	0.034	320	0.213
BE_3b	Facade area	0.034	342	0.170
BE_3c	Facade area	0.034	363	0.131
BE_3d	Facade area	0.031	274	0.194
BE_3e	Facade area	0.031	286	0.155
BE_3f	Facade area	0.031	317	0.119
BE_3g	Facade area	0.023	351	0.144
BE_3h	Facade area	0.023	391	0.115
BE_3i	Facade area	0.023	466	0.088
BE_4a	Facade area	0.031	353	0.194
BE_4b	Facade area	0.031	384	0.155
BE_4c	Facade area	0.031	415	0.119
BE_4d	Facade area	0.034	384	0.213
BE_4e	Facade area	0.034	415	0.170
BE_4f	Facade area	0.034	446	0.131
BE_5a	Cellar ceiling area	0.031	80	0.388
BE_5b	Cellar ceiling area	0.031	112	0.194
BE_6b	Window area		679	0.83
BE_6b	Window area		689	0.76

Table 10: Retrofit matrix for building envelopeSigrist (2018)

Chen, Y., T. Hong, and M. A. Piette (2017, November). Automatic generation and simulation of urban building energy models based on city datasets for city-scale building retrofit analysis. *Applied Energy 205*, 323–335.

De Rosa, M., V. Bianco, F. Scarpa, and L. A. Tagliafico (2014, September). Heating and cooling building energy demand evaluation; a simplified model and a modified degree days approach. *Applied Energy 128*, 217–229.

Deb, C., Z. Dai, and A. Schlueter (2021). A machine learning-based framework for cost-optimal building retrofit. *Applied Energy 294*, 116990.

Deb, C., M. Frei, J. Hofer, and A. Schlueter (2019, January). Automated load disaggregation for residences with electrical resistance heating. *Energy and Buildings 182*, 61–74. 00001.

Deb, C., M. Frei, and A. Schlueter (2020, January). Identifying temporal properties of building components and indoor environment for building performance assessment. *Building and Environment 168*, 106506. 00000.

Deb, C., L. Gelder, M. Spiekman, G. Pandraud, R. Jack, and R. Fitton (2021). Measuring the heat transfer coefficient (htc) in buildings: A stakeholder's survey. *Renewable and Sustainable Energy Reviews 144*, 111008.

Deb, C. and S. E. Lee (2018). Determining key variables influencing energy consumption in office buildings through cluster analysis of pre-and post-retrofit building data. *Energy and Buildings 159*, 228–245.

Deb, C. and A. Schlueter (2021). Review of data-driven energy modelling techniques for building retrofit. *Renewable and Sustainable Energy Reviews 144*, 110990.

Dong, B., C. Cao, and S. E. Lee (2005). Applying support vector machines to predict building energy consumption in tropical region. *Energy and Buildings 37*(5), 545–553.

Fan, C., F. Xiao, and S. Wang (2014). Development of prediction models for next-day building energy consumption and peak power demand using data mining techniques. *Applied Energy 127*, 1–10.

Foucquier, A., S. Robert, F. Suard, L. Stéphan, and A. Jay (2013). State of the art in building modelling and energy performances prediction: A review. *Renewable and Sustainable Energy Reviews 23*, 272–288.

Frei, M., C. Deb, R. Stadler, Z. Nagy, and A. Schlueter (2020, March). Wireless sensor network for estimating building performance. *Automation in Construction 111*, 103043. 00000.

Friedrich, L. and A. Afshari (2015). Short-term forecasting of the abu dhabi electricity load using multiple weather variables. *Energy Procedia 75*, 3014–3026.

Fumo, N. and M. R. Biswas (2015). Regression analysis for prediction of residential energy consumption. *Renewable and sustainable energy reviews 47*, 332–343.

Guardigli, L., M. A. Bragadin, F. Della Fornace, C. Mazzoli, and D. Prati (2018, May). Energy retrofit alternatives and cost-optimal analysis for large public housing stocks. *Energy and Buildings 166*, 48–59.

Guo, Y., J. Wang, H. Chen, G. Li, J. Liu, C. Xu, R. Huang, and Y. Huang (2018). Machine learning-based thermal response time ahead energy demand prediction for building heating systems. *Applied energy 221*, 16–27.

Guo, Z., K. Zhou, X. Zhang, and S. Yang (2018). A deep learning model for short-term power load and probability density forecasting. *Energy 160*, 1186–1200.

Hochreiter, S. and J. Schmidhuber (1997). Long short-term memory. *Neural Computation 9*(8), 1735–1780.

Jain, R. K., K. M. Smith, P. J. Culligan, and J. E. Taylor (2014). Forecasting energy consumption of multi-family residential buildings using support vector regression: Investigating the impact of temporal and spatial monitoring granularity on performance accuracy. *Applied Energy 123*, 168–178.

Lundberg, S. M. and S.-I. Lee (2017). A unified approach to interpreting model predictions. In I. Guyon, U. V. Luxburg, S. Bengio, H. Wallach, R. Fergus, S. Vishwanathan, and R. Garnett (Eds), *Advances in Neural Information Processing Systems 30*, pp. 4765–4774. Curran Associates, Inc.

Luong, M.-T., H. Pham, and C. D. Manning (2015). Effective approaches to attention-based neural machine translation. *arXiv preprint arXiv:1508.04025*.

Marino, D. L., K. Amarasinghe, and M. Manic (2016). Building energy load forecasting using deep neural networks. In *IECON 2016-42nd Annual Conference of the IEEE Industrial Electronics Society*, pp. 7046–7051. IEEE.

Massana, J., C. Pous, L. Burgas, J. Melendez, and J. Colomer (2015). Short-term load forecasting in a non-residential building contrasting models and attributes. *Energy and Buildings 92*, 322–330.

Rahman, A., V. Srikumar, and A. D. Smith (2018). Predicting electricity consumption for commercial and residential buildings using deep recurrent neural networks. *Applied energy 212*, 372–385.

Sigrist, D. (2018). Cost-optimal retrofit analysis for residential buildings. unpublished semester project.

Sigrist, D., C. Deb, M. Frei, and A. Schlüter (2019, November). Cost-optimal retrofit analysis for residential buildings. *Journal of Physics: Conference Series 1343*, 012030.

Srivastava, N., G. Hinton, A. Krizhevsky, I. Sutskever, and R. Salakhutdinov (2014). Dropout: a simple way to prevent neural networks from overfitting. *The Journal of Machine Learning Research 15*(1), 1929–1958.

Wang, Z., Y. Wang, R. Zeng, R. S. Srinivasan, and S. Ahrentzen (2018). Random forest based hourly building energy prediction. *Energy and Buildings 171*, 11–25.

Yuan, J., V. Nian, and B. Su (2019, November). Evaluation of cost-effective building retrofit strategies through soft-linking a metamodel-based Bayesian method and a life cycle cost assessment method. *Applied Energy 253*, 113573.

Zhao, H.-x. and F. Magoulès (2012). A review on the prediction of building energy consumption. *Renewable and Sustainable Energy Reviews 16*(6), 3586–3592.